Supplementary information

of

Electric field-driven one-step formation of vertical p–n junction TiO2 nanotubes exhibiting strong photocatalytic hydrogen production

Moonsu Kim[†,a], Jaewon Lee[†,b], Minyeong Je[†,c], Bumgi Heo[a], Hyeonseok Yoo[d], Heechae Choi[c,], Jinsub Choi[a,*] and Kiyoung Lee[b,e*]*

a: Department of Chemistry and Chemical Engineering, Inha University,
22212 Incheon, Republic of Korea
b: Department of Advanced Science and Technology Convergence, Kyungpook National University,
37224 Sangju, Gyeongsangbuk-do, Republic of Korea
c: Institute of Inorganic Chemistry, University of Cologne
50939 Cologne, Germany
d: Steel Solution Research Lab., POSCO
21985 Incheon, Republic of Korea
e: School of Nano & Materials Science and Engineering, Kyungpook National University,
37224 Sangju, Gyeongsangbuk-do, Republic of Korea

†: The authors are equally contributed.

*Corresponding authors.
E-mail: h.choi@uni-koeln.de (Heechae Choi), jinsub@inha.ac.kr (Jinsub Choi), kiyoung@knu.ac.kr (Kiyoung Lee)

Supplementary information note

In Supplementary information Scheme 1, the role of fluoride ion in the preparation of the TiO_2 nanotube array is comprehensively described. First, the applied potential between the working and counter electrodes formed dissolved metal ions and a barrier oxide layer on the substrate. Generally, the thickness of the oxide layer is proportional to the applied voltage, which is approximately 1.4 nm V^{-1}. Second, dissolved metal ions reacted with fluoride ion, thereby forming TiF_6^{2-}. They exhibited corrosion properties, such that the formed metal fluoride anions etched the surface of the barrier oxide layer, forming etched pits. Naked metal pits, resulting from the etching made by metal fluoride anions, were deposited into the barrier oxide layer, and this procedure was repeated during the application of the electric field. As a result, the anodic metal oxide structure grew on the substrate; thus, an anodic TiO_2 nanotube array was obtained [1]. For the experimental conditions, 20 V of applied voltage at room temperature for 4 h was used as electric field. With regard to the TiO_2 nanotube array, the nanostructure film, which was formed by the direct growth anodization without binding materials, was able to provide a catalyst with a physically and chemically extensive stable supporting structure, electron-hole pathway, and high surface area. Thereafter, high additive potential was conducted with the dopant-containing electrolyte. It is one of the methods of forcibly intercalating dopants into the TiO_2 nanotube array. After conducting high additive potential, the doped TiO_2 nanotube array was obtained, with an additional grown barrier layer under the array because additional voltage was applied after anodization, such that the barrier oxide layer was additionally coated again, similar to that shown in Supplementary information Schemes 1 and 2.

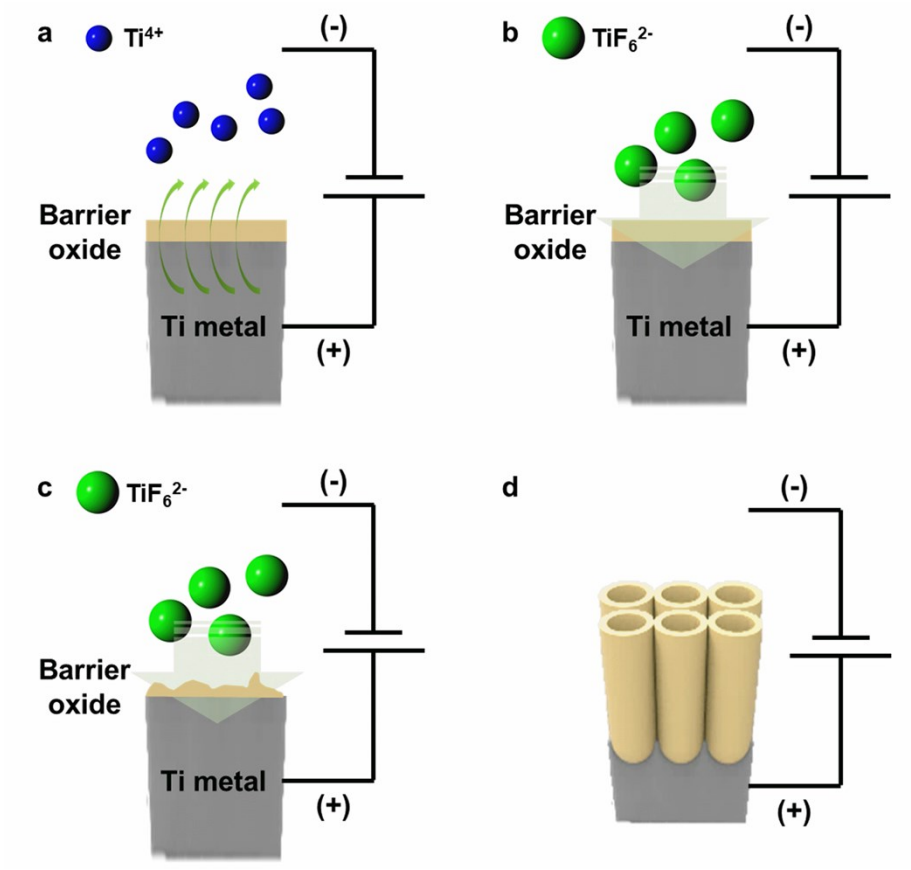

Supplementary information Scheme 1. General mechanism describing anodization process.

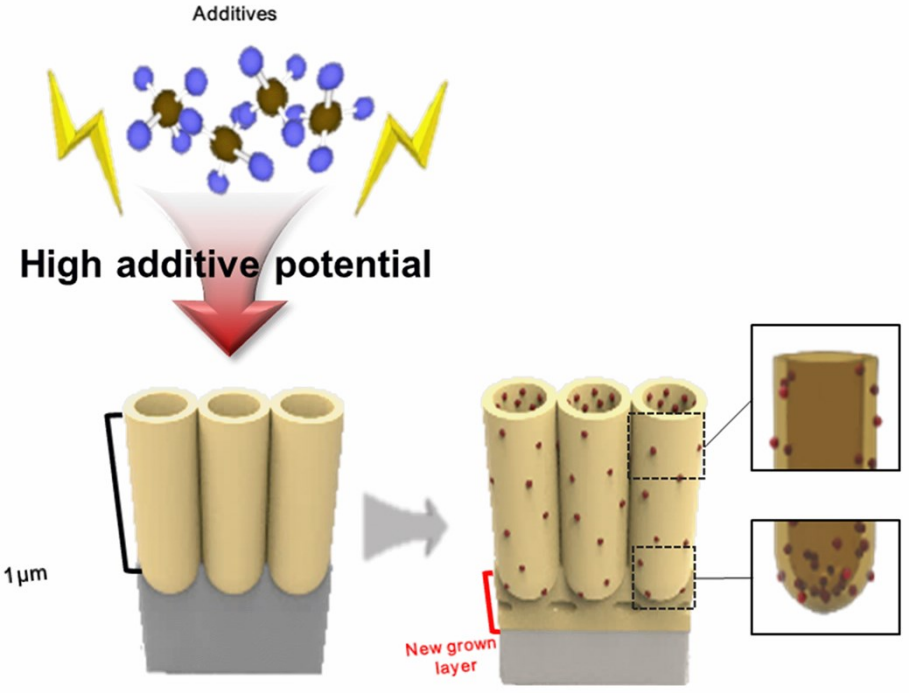

Supplementary information Scheme 2. Additive doping with high additive potential.

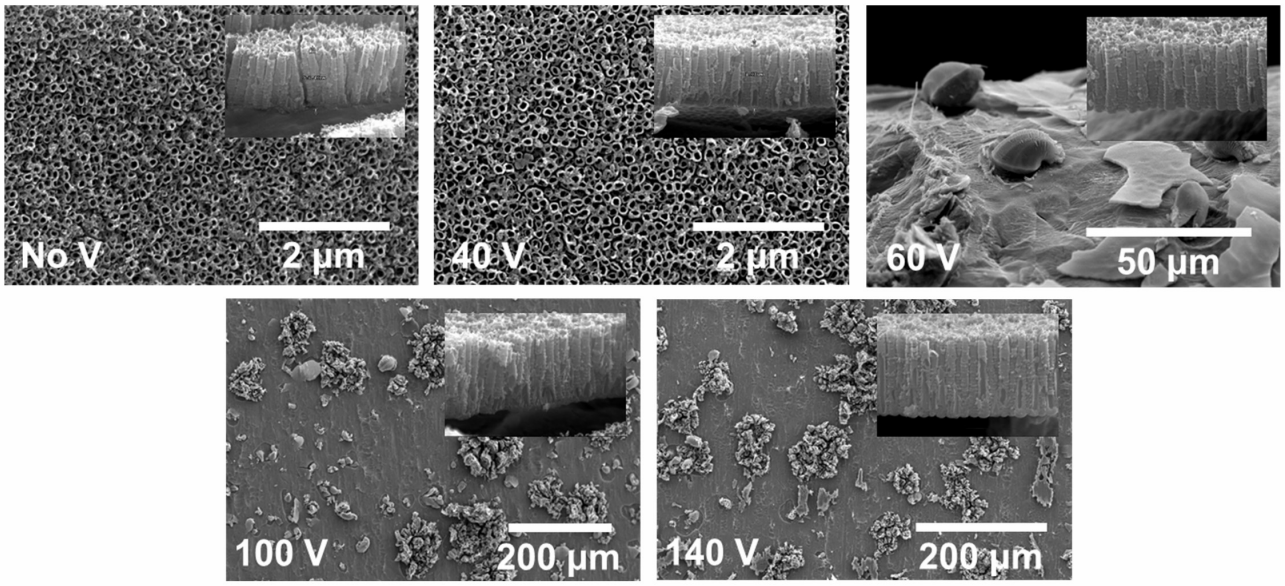

Supplementary information Figure 1. SEM images of Pd-doped TiO_2 nanotube array at the various applied high additional voltage levels. Inlets exhibit each cross-sectional view.

In Figure S1, small pits manifested on the surface. This phenomenon is referred to as the rapid breakdown anodization caused by chloride ions because the etching properties of chloride are stronger than those of fluoride, such that the products of rapid breakdown anodization are usually nanotube bundle powders[2, 3]. Notably, however, the TiO_2 nanotube bundle did not manifest after the coating of the nanotube array because the previously prepared TiO_2 nanotube array probably protected the Ti substrate. Therefore, despite the chloride ion and high applied voltage, the TiO_2 nanotube array had been maintained even after a high additional voltage was applied. Well-taken cross-sectional views were sufficient evidence in determining that the TiO_2 nanotube array was maintained.

TOF-SIMS was carried out to detect the depth of the Pd-doped region. Therefore, initially, the TiO_2 nanotube array had to be detached from the substrate so that the epoxy polymer was allowed to be employed as a detacher agent. The detachment of the TiO_2 nanotube array is described below in detail in Figure S2[4].

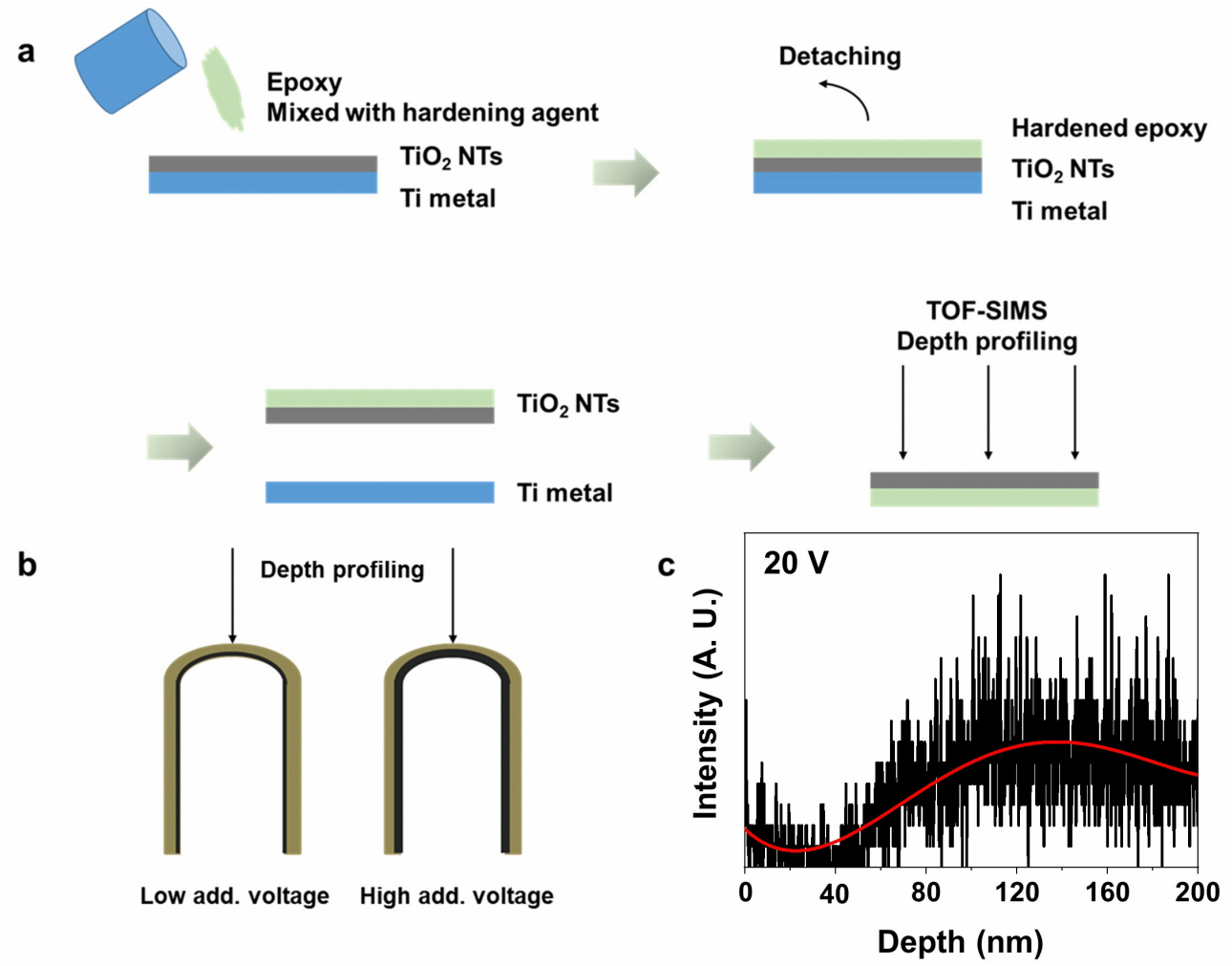

Supplementary information Figure 2. (a), (b) Procedure of detaching the TiO_2 nanotube array from the substrate. (c) Mass spectrum of the Pd-doped TiO_2 nanotube array with the applied electric field of 20 V.

Considering that Pd species were not dispersed deeply at the low additional electric field, it was not detected at an early time by TOF-SIMS. Pd was belatedly detected, meaning that the Pd was not well-injected into the bottom region[5]. Therefore, TOF-SIMS from the bottom to the inside is a more suitable method for the purpose of analyzing the formation of heterojunction TiO_2 nanotube array via the high additional electric field method. For example, TOF-SIMS can give information that the Pd-doped TiO_2 nanotube array has a high Pd species region at the bottom side from when it was detected. At a high additional electric field of 100 V, it can start detecting a small amount of Pd at the bottom region. Therefore, the vertical *p–n* junction was formed after the application of the high additional electric field of 100 V. With the high electric field, the concentration of Pd was increased (Figure S3).

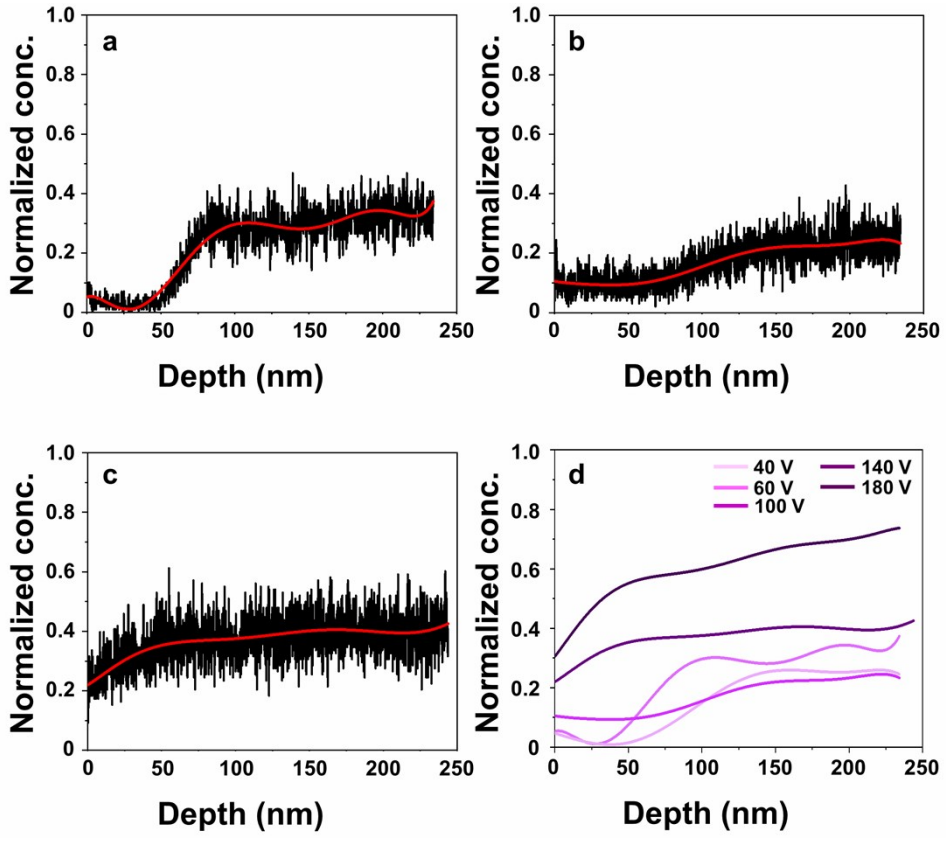

Supplementary information Figure 3. The results of TOF-SIMS depth profile mass spectrum of the Pd-doped TiO_2 nanotube array with different applied high additional electric field. (a) 40 V doped, (b) 100 V doped, (c) 140 V doped, and (d) comparison of the samples by fitted curves.

Using the results of the calculations, the phenomenon which occurred in the TiO_2 nanotube array can be predicted with supercell model (Figure S4), as described in Figure S5. With optimum bias on the Ti electrode, a vertical *p*–*n* junction was formed and the entire TiO_2 nanotube had band bending as the charge carriers became depleted, an ideal condition for maximum photocatalytic activity (*top panel*). When the bias was small, there was a flat band area at the top of the TiO_2 (*middle panel*); hence, the photocatalytic activity was lower than that of the optimum bias. When the bias was too large, the entire or large portion of the grown TiO_2 nanotube was expected to become *p*-type (*bottom panel*). Thus, it was not suitable for water oxidation.

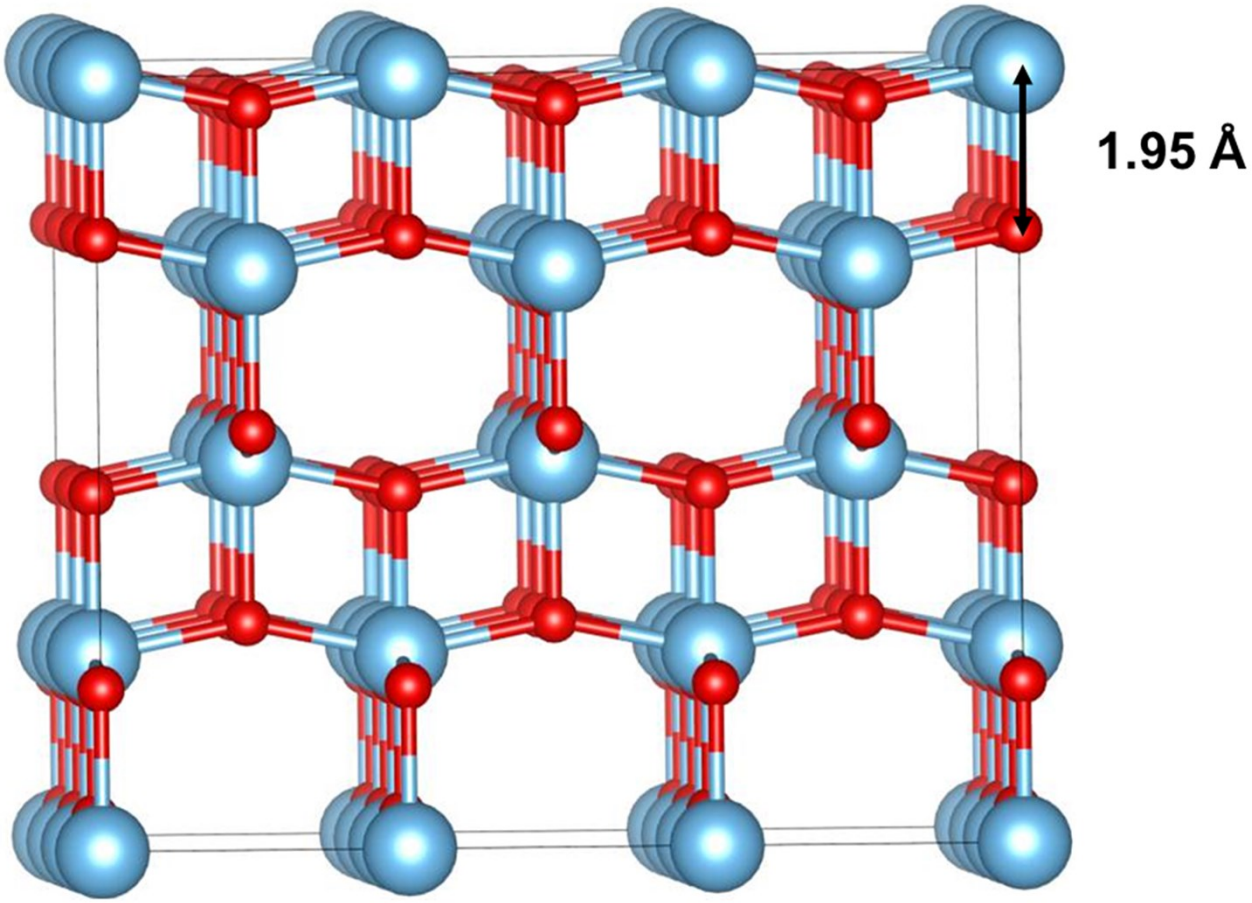

Supplementary information Figure 4. Calculated phase space of TiO_2 and TiClO, which is expressed as the function of chemical potentials of Cl and O, considering the varying atmospheric conditions during the syntheses

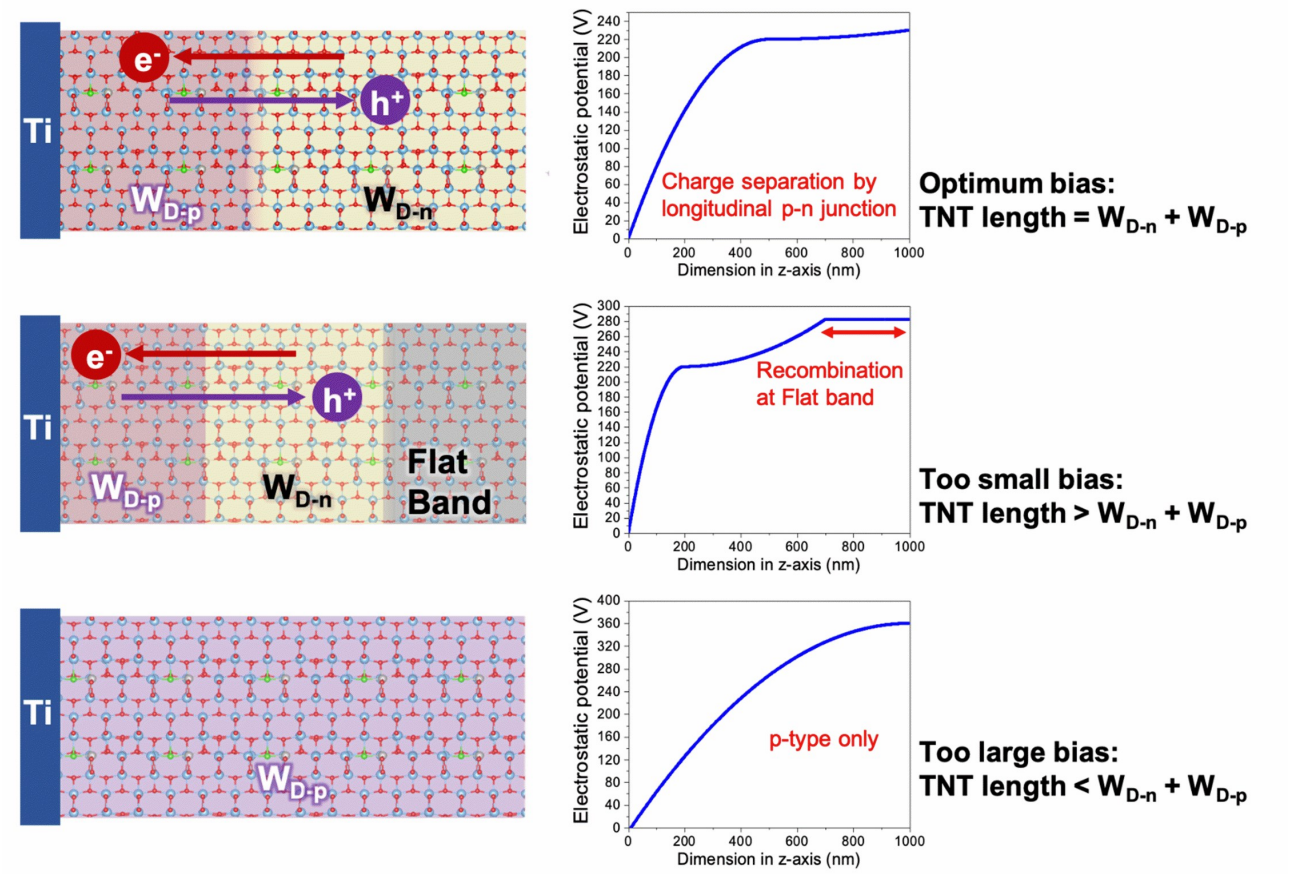

Supplementary information Figure 5. Band bending with magnitudes of bias and charge densities in the TiO_2 nanotube array.

The valence edge of the *n*-type TiO_2 was well known as 2.6 to 2.8 eV[6-9]. Thus, the valence band edge of the top region of the TiO_2 nanotube array was determined as 2.8 eV, similar to that of the *n*-type TiO_2. Likewise, the valence edge of the bottom region (*p*-type region) can be predicted and measured using the same method as that used in Figure S2 and S3, with the TOF-SIMS-depth profile. These results showed the change in the valence band edge of the *p*- and *n*-type regions, which was 0.4 and 2.8 eV, respectively (Figure S6).

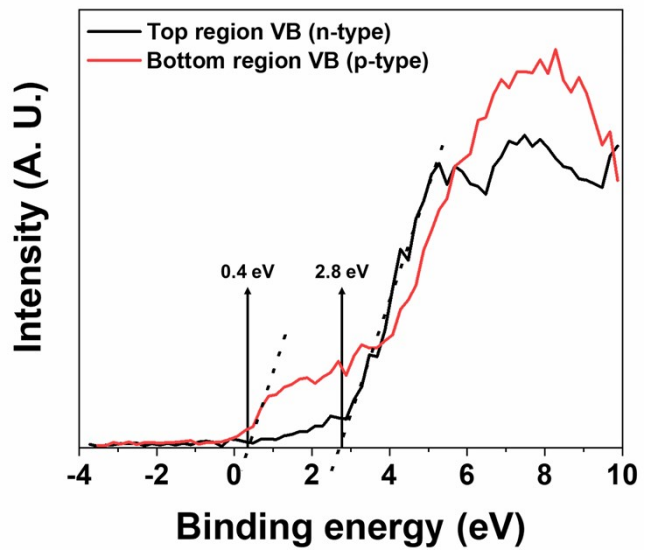

Supplementary information Figure 6. Results of probing valence band edge at the top region (*n*-type) and bottom region (*p*-type) using XPS for the detection of low binding energy.

Generally, the more catalyst concentration is detected below limitation, the more catalytic effect occurs; thus, it can be expected that more Pd concentration is detectable with the high additional electric field. However, the saturation region and highest concentration manifested at the low additional electric field, a condition of underpotential deposition[5]. Underpotential deposition was reported by Kim et al. It is similar to electrophoresis because applied voltage is low and anion species are attracted to the surface of the TiO_2 nanotube array. However, at a high additional electric field, doped amount is decreased. The reason is that the Pd precursor, $PdCl_6^{2-}$, is strongly aggressive, such that some amount precursor is used as a dopant and the others probably etch the TiO_2 nanotube array, leading to rapid breakdown anodization. Despite the separation of their roles, the doped amount of Pd was limited to approximately 0.0075 mg, however, it was well-injected into the bottom region of the TiO_2 nanotube array, thereby forming the vertical *p–n* junction. Therefore, despite the limiting amount of Pd, the doped TiO_2 nanotube array at a high additional electric field showed higher performance than that at the low additional electric field (Figure S7).

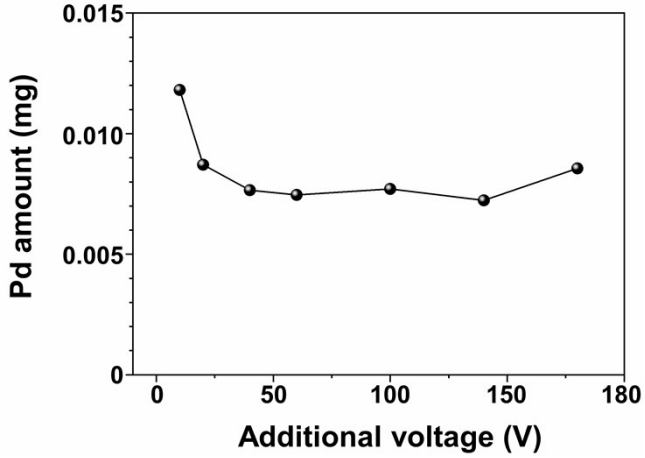

Supplementary information Figure 7. Overall amount of Pd in TiO_2 nanotube array determined via ICP-MS.

References

1 K. Lee, A. Mazare, P. Schmuki, *Chem. Rev.,* 2014, **114**(19), 9385–9454, DOI: https://doi.org/10.1021/cr500061m.

2 R. P. Antony, T. Mathews, A. Dasgupta, S. Dash, A. K. Tyagi, B. Raj, *J. Solid State Chem.,* 2011, **184**(3), 624-632, DOI: http://doi.org/10.1016/j.jssc.2011.01.020.

3 S. Kim, M. Seong, J. Choi, *J. Electrochem. Soc.,* 2015, **162**(6), C205-C208, DOI: http://doi.org/10.1149/2.0291506jes.

4 N. Y. Kim, G. Lee, J. Choi, *Chem. Eur.,* 2018, **24**(71), 19045–19052, DOI: https://doi.org/10.1002/chem.201804313.

5 S. Kim, H. Yoo, O. Rhee, J. Choi, *J. Phys. Chem. C,* 2015, **119**(37), 21497–21503, DOI: https://doi.org/10.1021/acs.jpcc.5b05790.

6 X. Chen, L. Liu, P. Y. Yu, S. S. Mao, *Science,* 2011, **331**(6018), 746–750, DOI: https://doi.org/10.1126/science.1200448.

7 M. Bledowski, L. Wang, A. Ramakrishnan, O. V. Khavryuchenko, *Phys. Chem. Chem. Phys.,* 2011, **13**(48), 21511–21519, DOI: https://doi.org/10.1039/c1cp22861g.

8 D. O. Scanlon, C. W. Dunnill, J. Buckeridge, S. A. Shevlin, A. J. Logsdail, S. M. Woodley, C. R. A. Catlow, M. J. Powell, R. G. Palgrave, I. P. Parkin, G. W. Watson, T. W. Keal, P. Sherwood, A. Walsh, A. A. Sokol, *Nat. Mater.,* 2013, **12**, 798–801, DOI: https://doi.org/10.1038/nmat3697.

9 N. Serpone, *J. Phys. Chem. B,* 2006, **110**(48), 24287–24293, DOI: https://doi.org/10.1021/jp065659r.